2021 43rd Annual International Conference of the
IEEE Engineering in Medicine & Biology Society (EMBC)
Oct 31 - Nov 4, 2021. Virtual Conference

2021 43rd Annual International Conference of the IEEE Engineering in Medicine & Biology Society (EMBC) | 978-1-7281-1179-7/21/$31.00 ©2021 IEEE | DOI: 10.1109/EMBC46164.2021.9629932

Axonal Conduction Delay Shapes the Precision of the Spatial Hearing in A Spiking Neural Network Model of Auditory Brainstem

Ben-Zheng Li, *Member*, *IEEE*, Sio Hang Pun, *Member*, *IEEE*, Mang I Vai, *Senior Member*, *IEEE*, Achim Klug, and Tim C. Lei

***Abstract*—One method by which the mammalian sound localization pathway localizes sound sources is by analyzing the microsecond-level difference between the arrival times of a sound at the two ears. However, how the neural circuits in the auditory brainstem precisely integrate signals from the two ears, and what the underlying mechanisms are, remains to be understood. Recent studies have reported that variations of axon myelination in the auditory brainstem produces various axonal conduction velocities and sophisticated temporal dynamics, which have not been well characterized in most existing models of sound localization circuits. Here, we present a spiking neural network model of the auditory brainstem to investigate how axon myelinations affect the precision of sound localization. Sound waves with different interaural time differences (ITDs) are encoded and used as stimuli, and the axon properties in the network are adjusted, and the corresponding axonal conduction delays are computed with a multi-compartment axon model. Through the simulation, the sensitivity of ITD perception varies with the myelin thickness of axons in the contralateral input pathways to the medial superior olive (MSO). The ITD perception becomes more precise when the contralateral inhibitory input propagates faster than the contralateral excitatory input. These results indicate that axon myelination and contralateral spike timing influence spatial hearing perception.**

I. Introduction

The ability to locate the origin of sounds is critical for animals to survive in the wild. The sound localization pathway is involved not only in sound localization per se but also our ability to separate a sound source of interest from background noises [1]. Alterations in this pathway in a number of medical conditions such as autism or one form of age-related hearing loss disallow an affected person to function in such environments. It is therefore imperative to study both the healthy localization pathway in order to better understand it, such that we can properly evaluate the effects that alterations have on the functioning of the circuit. In mammalian hearing, sound localization is achieved by analyzing intensity and time differences that the same sound produces when arrives at the two ears. These interaural intensity and time differences vary systematically along the azimuth, providing a neural interpretation for the sound localization circuit to pinpoint the sound origin on the azimuth. Interaural intensity differences are suitable to localize high-frequency sounds, which interaural time differences are suitable to localize low frequencies. This report focuses on the latter binaural neurons in which medial superior olive (MSO) process interaural time differences (ITDs) of low frequency sounds over a microsecond-order timescale, making this neural circuit one of the most temporally precise neuronal circuits in the mammalian brain [1] [2]. During this process, the neural activity generated from the two cochleae propagates initially in separate monaural neural circuits and eventually converges onto binaural neurons in the MSO. How the sound localization circuit accomplishes the micro-second precise integration of the two sets of signals across multiple fiber bundles, synapses, and neuronal types, is not entirely clear [1] [3].

For a precise coincidence detection, action potential timing needs to be well tuned, despite there are several internal delays generated in the sound localization circuit. These include cochlear delays, synaptic delays, post-synaptic integration delays, and spike propagation delays [2]-[4]. Interestingly, some studies observed that the contralateral excitatory and inhibitory inputs to MSO differ in their axon morphology and conduction velocity [2] [4] [5], suggesting that these axons and contralateral propagation delays in the circuit might be specifically tuned to input timing and may contribute to the spatial hearing perception [3].

On the one hand, the contributions of precise contralateral inhibition to ITD coding have been investigated in several existing models of single MSO neurons [6]-[9], but these studies largely focused on the post-synaptic integration and cellular morphology in MSO neurons rather than an analysis of other involved nuclei and projections in the circuit. Additionally, previous network models of mammalian sound localization circuits [10] [11] commonly symbolized the propagation delays as a constant without considering the differences in axon morphology; they also simplified the medial nucleus of the trapezoid body (MNTB) as a simple relay, making these models incapable of handling detailed temporal dynamics. Some other network models [12] [13]

* Research supported by the Science and Technology Development Fund, Macau SAR (File no. 088/2016/A2, 0144/2019/A3, 0022/2020/AFJ, SKL-AMSV (FDCT-funded), SKL-AMSV-ADDITIONAL FUND, SKL-AMSV(UM)-2020-2022), the University of Macau (File no. MYRG2018-00146-AMSV, MYRG2019-00056-AMSV), and the National Key R&D Program of China (No. 2020YFB1313502).

Ben-Zheng Li is with the State Key Laboratory of Analog and Mixed-Signal VLSI, University of Macau, Macau, and with the Department of Physiology and Biophysics, University of Colorado Anschutz Medical Campus, Aurora, CO 80045 USA.

Sio Hang Pun is with the State Key Laboratory of Analog and Mixed-Signal VLSI, University of Macau, Macau.

Mang I Vai is with the State Key Laboratory of Analog and Mixed-Signal VLSI, and with the Department of Electrical and Computer Engineering, Faculty of Science, University of Macau, Macau.

Achim Klug is with the Department of Physiology and Biophysics, University of Colorado Anschutz Medical Campus, Aurora, CO 80045 USA.

Tim C. Lei (corresponding author) is with the Department of Electrical Engineering, University of Colorado Denver, Denver, CO 80204 USA. (e-mail: tim.lei@ucdenver.edu)

tuned spike timing through the propagation delays, but their models employed the delay line structure mimicking the Jeffress model which is inconsistent with in-vivo data in mammals [6].

To investigate how those axonal properties and action potential timings affect sound localization precision, we developed a spiking neural network (SNN) model of the mammalian auditory brainstem with a more detailed architecture and variable axon myelination patterns. Through the simulation, we found that the axon myelination in contralateral pathways to MSO influences ITD perception sensitivity. The relatively thicker myelin in the contralateral inhibitory pathway makes the travel of the contralateral inhibition faster than the excitation, and this leading contralateral inhibition results in a more precise sound localization perception.

II. Methods

A. Network Architecture

The sound localization circuit in the mammalian auditory brainstem contains several neural processing centers, as shown in Fig. 1a. The cochlea nuclei (CN) receive the cochlear responses to acoustic stimulation through the auditory nerve (AN). The spherical bushy cells (SBCs) in the CN excite the ipsilateral lateral superior olive (LSO) and both bilateral medial superior olives (MSO). The medial nucleus of the trapezoid body (MNTB) receives excitatory input from the globular bushy cells (GBCs) in the contralateral CN and sends inhibitory projections to the ipsilateral LSO and MSO. Besides, MSO also receives an ipsilateral inhibitory input from the lateral nucleus of the trapezoid body (LNTB) driven by the GBCs. For binaural cues, the MSO processes microsecond differences in the arrival time of low-frequency sounds, i.e., interaural time difference (ITD), and requires higher precision of spike timing comparing to the LSO that computes the interaural level difference (ILD) of high-frequency sounds [2].

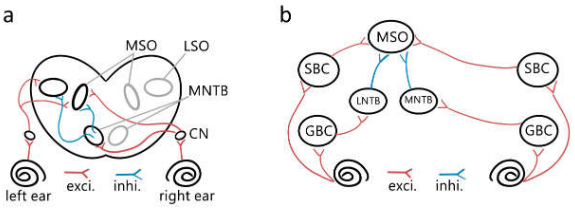

Figure 1. Circuit schematics of (a) mammalian sound localization circuits in auditory brainstem; (b) the SNN model for ITD detection.

The architecture of the proposed SNN model (Fig. 1b) consists of MSO and involved nuclei. Each neuron group consists of 1000 spiking neurons with the characteristic frequency equal to the frequency of the sound stimuli. The detailed parameters of the architecture are listed in Table.I. Neurons between different neural populations were randomly connected with certain probabilities taken from previous studies [11] [14] [15].

The spike generators in AN stimulate the network with the encoded sound signals. Those signals were made from 300 Hz 50 dB SPL (sound pressure level) pure tones lasting 100 ms with 20 ms ramp-up and ramp-down, and released to two ears at different times with ITDs ranging from -1 to +1 ms. A peripheral hearing model [16] [17] was used to encode the sound waves into the AN's neural activities. The AN composites auditory nerve fibers in three spontaneous firing rates with a proportional ratio of 6:2:2 for high, medium, and low spontaneous rate fibers.

TABLE I. List of Parameters for Network Architecture

Population	*Type*	*Connection*	*Connectivity*
AN	Spike generator	AN → ipsi. GBC AN → ipsi. SBC	4 % 4 %
SBC	Excitatory	SBC → ipsi. MSO SBC → cont. MSO	0.6 % 0.6 %
GBC	Excitatory	GBC → ipsi. LNTB GBC → cont. MNTB[a]	0.6 % 0.1 %
MNTB	Inhibitory	MNTB → ipsi. MSO	0.3 %
LNTB	Inhibitory	LNTB → ipsi. MSO	0.6 %
MSO	Excitatory		

a. calyx of held with $\Delta g_{e,GBC\rightarrow MNTB}$ = 100 nS; ipsi.: ipsilateral; cont.: contralateral

B. Neurons and Synapses

Spiking neurons in the network were formulated using a conductance-based leaky integrate-and-fire model with membrane potential (v_m) described by a differential equation:

$$C_m \frac{dv_m}{dt} = g_l(E_l - v_m) + I_{syn} \quad (1)$$

where C_m is the membrane capacitance, I_{syn} is the synaptic current, g_l is the leaky conductance, and E_l is the leak reversal potential. When the membrane potential reaches the firing threshold V_{th} , the cell elicits an action potential, and its membrane potential is reset to V_{reset} that remains for a refractory period τ_{ref}. The synaptic current I_{syn} is given by the following equations:

$$I_{syn} = g_e(E_e - v_m) + g_i(E_i - v_m) \quad (2)$$

$$\tau_{e,i} \frac{dg_{e,i}}{dt} = -g_{e,i} \quad (3)$$

where E_e and E_i are the excitatory and inhibitory reversal potentials, g_e and g_i are the conductance of excitatory and inhibitory synapses that exponentially decays with the time constants of τ_e and τ_i, respectively. Each action potential induces an increment of postsynaptic conductance, Δg_e or Δg_i, regarding the cell type. All used parameters are summarized in Table.II.

TABLE II. List of Parameters for Neuron and Synapes

Parameter	*Value*	*Parameter*	*Value*
C_m	70 pF	E_e	0 mV
V_{th}	-50 mV	E_i	-70 mV
V_{reset}	-55.8 mV	Δg_e	15 nS
τ_{ref}	5 ms	Δg_i	55 nS
E_l	-55.9 mV	τ_e	0.23 ms
g_l	13 nS	τ_i	2 ms

The ipsilateral connections include a normally distributed synaptic delay of 0.4 ± 0.05 ms (mean ± standard deviation), and the contralateral connections traveling across the midline involves axonal conduction delays computed from different myelination properties using a multi-compartment axon model [4] [18].

C. Data Analysis

Responses of a neuron to ITDs were represented as the firing rate during the sound stimulation. Moreover, each neuron's ITD responses were smoothed using a Gaussian filter with a window of +/-100 μs ITDs. The simulation was repeated 30 times with different random seeds to compensate for the random effects induced during the sound stimuli encoding and the network connection. The nucleus's ITD response was computed as the mean ITD responses of all neurons from the nucleus across all random permutations.

The sensitivity to ITDs was estimated by the just noticeable difference (JND) which describes the shortest perceptible change of ITDs. The JNDs are calculated by comparing responses between symmetric ITDs, e.g. +/- 20 μs. The difference of firing rates between left and right MSOs under symmetric ITDs were computed for each random permutation and then compared using a one-tailed Mann-Whitney U test. The JND was defined as the smallest ITD that reaches the minimum significance.

III. Results

To elucidate the relationship between axon myelinations and conduction delays, the conduction velocities were computed under various internode lengths (L) and myelin thicknesses (d). The results in Fig. 2 show that the conduction velocity is proportional to the thickness of the myelin sheath. The myelin thickness was tuned under a fixed internode length (L = 0.2 mm) to obtain different axon conduction velocities in the following analyses.

The results of network simulation indicate that the ITD perception is more precise when the GBC fiber has thicker myelin comparing to the SBC fiber, and the contralateral inhibition propagates faster than the excitation (shown in Fig. 3). For details, the axon myelination of SBC and GBC fibers influences the ITD perception in different ways. The peak amplitude and location of ITD tuning curves vary with the myelin thickness of SBC fiber and the peak width changes with GBC fiber.

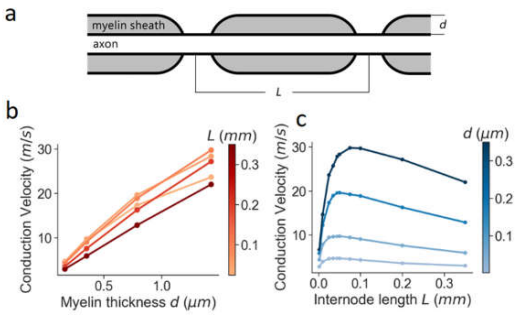

Figure 2. Axon myelination and conduction velocity: (a) schematic of axon myelination; (b) axonal conduction velocity versus myelination thickness; (c) axonal conduction velocity versus internode length.

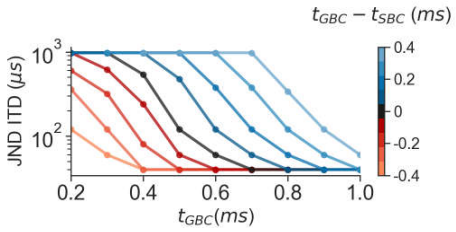

Figure 4. The JNDs of the ITD versus different axonal synaptic delays of from contralateral GBC and SBC fibers; red lines indicate the leading inhibition; the black line indicates equal propagation delays; the blue lines indicate the lagging inhibition.

The sensitivity of ITD perception was changed while altering contralateral spike timing. Taken the difference of delays between SBC and GBC fibers as $dt = t_{GBC} - t_{SBC}$, the leading contralateral inhibition case, i.e. $dt < 0$, produced

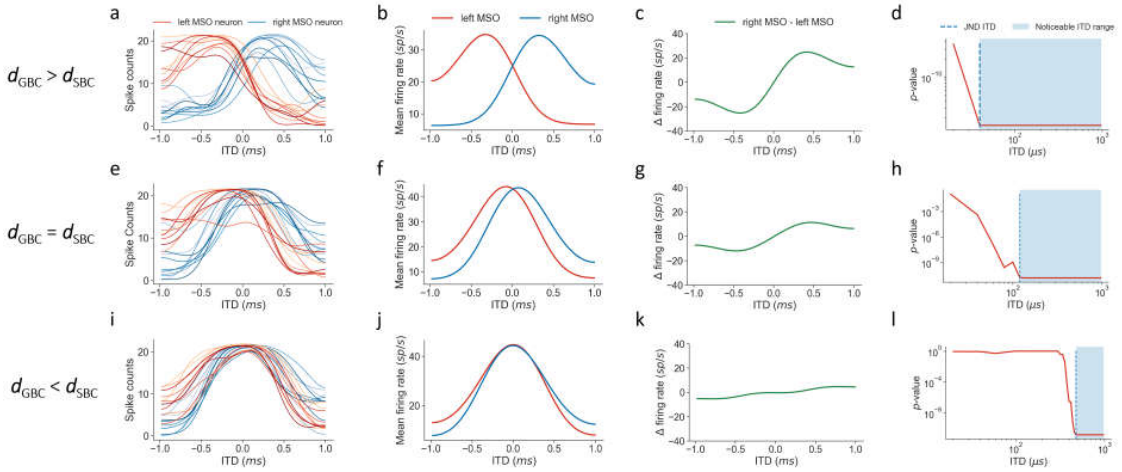

Figure 3. Neural responses to ITDs differs from the relative myelin thickness: (a-d) neural responses with thicker GBC fiber myelin (d_{SBC} = 0.165 μm, d_{GBC} = 0.487 μm); (e-h) neural responses with equal myelin thickness (d_{SBC} = d_{GBC} = 0.487 μm); (i-l) neural responses with thicker SBC fiber myelin (d_{SBC} = 1.032 μm and d_{GBC} = 0.487 μm). Listed responses includes the MSO neuronal ITD responses (a, e, i), ITD tuning curves (b, f, j), differences of firing rates between right and left MSO (c, g, k), and the noticeable ITD ranges (d, h, l).

smaller JNDs of the ITD and more sensitive ITD perception (Fig.4).

IV. Discussion

The computational modeling results illustrate the influence of axon properties and contralateral spike timing on the ITD perception, supporting the critical role of axon myelination and contralateral inhibition in ITD tuning at the circuit-level.

In our model, the conduction velocities of contralateral inputs to MSO were tuned by adjusting the myelin thickness on contralateral projections. With the thicker myelin layers on the GBC projection, the contralateral inhibition precedes the excitation, and the ITD responses became more sensitive and precise. This result is consistent with previous experimental and computational findings at the cellular level [2] [4] [6] [7] [9] and implies the axonal morphological adaptation on the contralateral inhibitory pathway accelerating the inhibition and modulating the ITD precision.

Our current model only discusses pure-tone stimulation with a single frequency and intensity level. How much the observed phenomenon would be affected by multiple frequencies and sound levels remains to be tested. The model will be further developed with the Hodgkin-Huxley-based neuron model to analyze the sound localization circuit's temporal dynamics under more complicated settings, as the previous studies had also reported the implementation of spiking neural models under complex sound stimuli like speeches [11] and reverberating echoes [19].

V. Conclusion

The effects of axon properties and spike timing on spatial hearing perception have been examined using the proposed SNN model of the auditory brainstem. The simulation results indicate that the axon myelination and propagation delays on the contralateral pathways to the MSO shaped the ITD tuning. The thicker myelin layers on the contralateral inhibitory pathway speed up the contralateral inhibition and sharpen the precision of ITD perception.

Acknowledgment

This work utilized the Summit supercomputer, which is supported by the National Science Foundation (awards ACI-1532235 and ACI-1532236), the University of Colorado Boulder, and Colorado State University. The Summit supercomputer is a joint effort of the University of Colorado Boulder and Colorado State University.

References

[1] B. Grothe, M. Pecka, and D. McAlpine, "Mechanisms of Sound Localization in Mammals," *Physiological Reviews*, vol. 90, no. 3, pp. 983–1012, Jul. 2010, doi: 10.1152/physrev.00026.2009.

[2] A. Stange-Marten *et al.*, "Input timing for spatial processing is precisely tuned via constant synaptic delays and myelination patterns in the auditory brainstem," *Proceedings of the National Academy of Sciences*, vol. 114, no. 24, pp. E4851–E4858, May 2017, doi: 10.1073/pnas.1702290114.

[3] B. Grothe, C. Leibold, and M. Pecka, "The Medial Superior Olivary Nucleus," *The Oxford Handbook of the Auditory Brainstem*, pp. 300–328, Dec. 2018, doi: 10.1093/oxfordhb/9780190849061.013.9.

[4] M. C. Ford *et al.*, "Tuning of Ranvier node and internode properties in myelinated axons to adjust action potential timing," *Nature Communications*, vol. 6, no. 1, Aug. 2015, doi: 10.1038/ncomms9073.

[5] A. H. Seidl, E. W. Rubel, and D. M. Harris, "Mechanisms for Adjusting Interaural Time Differences to Achieve Binaural Coincidence Detection," *Journal of Neuroscience*, vol. 30, no. 1, pp. 70–80, Jan. 2010, doi: 10.1523/jneurosci.3464-09.2010.

[6] A. Brand, O. Behrend, T. Marquardt, D. McAlpine, and B. Grothe, "Precise inhibition is essential for microsecond interaural time difference coding," *Nature*, vol. 417, no. 6888, pp. 543–547, May 2002, doi: 10.1038/417543a.

[7] Y. Zhou, "A Model for Interaural Time Difference Sensitivity in the Medial Superior Olive: Interaction of Excitatory and Inhibitory Synaptic Inputs, Channel Dynamics, and Cellular Morphology," *Journal of Neuroscience*, vol. 25, no. 12, pp. 3046–3058, Mar. 2005, doi: 10.1523/jneurosci.3064-04.2005.

[8] A. Brughera, L. Dunai, and W. M. Hartmann, "Human interaural time difference thresholds for sine tones: The high-frequency limit," *The Journal of the Acoustical Society of America*, vol. 133, no. 5, pp. 2839–2855, May 2013, doi: 10.1121/1.4795778.

[9] M. H. Myoga, S. Lehnert, C. Leibold, F. Felmy, and B. Grothe, "Glycinergic inhibition tunes coincidence detection in the auditory brainstem," *Nature Communications*, vol. 5, no. 1, pp. 1–13, May 2014, doi: 10.1038/ncomms4790.

[10] L. Wang, S. Devore, B. Delgutte, and H. S. Colburn, "Dual sensitivity of inferior colliculus neurons to ITD in the envelopes of high-frequency sounds: experimental and modeling study," *Journal of Neurophysiology*, vol. 111, no. 1, pp. 164–181, Jan. 2014, doi: 10.1152/jn.00450.2013.

[11] J. Encke and W. Hemmert, "Extraction of Inter-Aural Time Differences Using a Spiking Neuron Network Model of the Medial Superior Olive," *Frontiers in Neuroscience*, vol. 12, Mar. 2018, doi: 10.3389/fnins.2018.00140.

[12] B. Glackin, J. A. Wall, T. M. McGinnity, L. P. Maguire, and L. J. McDaid, "A spiking neural network model of the medial superior olive using spike timing dependent plasticity for sound localization," *Frontiers in Computational Neuroscience*, 2010, doi: 10.3389/fncom.2010.00018.

[13] Z. Pan, M. Zhang, J. Wu, and H. Li, "ulti-Tones' Phase Coding (MTPC) of Interaural Time Difference by Spiking Neural Network," *arXiv preprint*, vol. arXiv:2007.03274, 2020.

[14] G. A. Spirou, J. Rager, and P. B. Manis, "Convergence of auditory-nerve fiber projections onto globular bushy cells," *Neuroscience*, vol. 136, no. 3, pp. 843–863, Jan. 2005, doi: 10.1016/j.neuroscience.2005.08.068.

[15] K. Couchman, B. Grothe, and F. Felmy, "Medial Superior Olivary Neurons Receive Surprisingly Few Excitatory and Inhibitory Inputs with Balanced Strength and Short-Term Dynamics," *Journal of Neuroscience*, vol. 30, no. 50, pp. 17111–17121, Dec. 2010, doi: 10.1523/jneurosci.1760-10.2010.

[16] M. S. A. Zilany, I. C. Bruce, and L. H. Carney, "Updated parameters and expanded simulation options for a model of the auditory periphery," *The Journal of the Acoustical Society of America*, vol. 135, no. 1, pp. 283–286, Jan. 2014, doi: 10.1121/1.4837815.

[17] M. Rudnicki, O. Schoppe, M. Isik, F. Völk, and W. Hemmert, "Modeling auditory coding: from sound to spikes," *Cell and Tissue Research*, vol. 361, no. 1, pp. 159–175, Jun. 2015, doi: 10.1007/s00441-015-2202-z.

[18] J. A. Halter and J. W. Clark, "A distributed-parameter model of the myelinated nerve fiber," *Journal of Theoretical Biology*, vol. 148, no. 3, pp. 345–382, Feb. 1991, doi: 10.1016/s0022-5193(05)80242-5.

[19] A. Brughera, J. Mikiel-Hunter, M. Dietz, and D. McAlpine, "Auditory brainstem models: adapting cochlear nuclei improve spatial encoding by the medial superior olive in reverberation," *bioRxiv*, vol. 694356, 2020.